

Study of the $(\text{Ca}_{1-x}\text{Sr}_x)\text{RuO}_3$ System with Nano-Crystals Prepared by the Solid-State Reaction Method

Adolfo Quiroz^{1,2*}, Elizabeth Chavira², José Eduardo Espinosa¹,
Rodolfo Palomino-Merino¹, Ernesto Esteban Marinero³, Masaya Nishioka⁴,
Valentín García-Vázquez⁵

¹Facultad de Ciencias Físico-Matemáticas, Postgrado en Física Aplicada, Benemérita Universidad Autónoma Puebla, Ciudad Universitaria, Puebla, México

²Instituto de Investigaciones en Materiales, Universidad Nacional Autónoma de México, México, D.F., México

³Purdue University, West Lafayette, IN, USA

⁴Hitachi San José Research Center, San José, California, USA

⁵Instituto de Física LRT, Benemérita Universidad Autónoma de Puebla, Puebla, México

Email: *adquiroz@hotmail.com, chavira@unam.mx, espinosa@fcfm.buap.mx, palomino@fcfm.buap.mx,
emarinero@purdue.edu, masaya.hishioka@hitachigst.com, meho@live.com.mx

Received 30 October 2014; revised 26 November 2014; accepted 16 December 2014

Copyright © 2015 by authors and Scientific Research Publishing Inc.

This work is licensed under the Creative Commons Attribution International License (CC BY).

<http://creativecommons.org/licenses/by/4.0/>



Open Access

Abstract

We present a study of their structure, morphology, electrical and magnetic properties on the $(\text{Ca}_{1-x}\text{Sr}_x)\text{RuO}_3$ system for $x = 0.0, 0.07, 0.10, 0.15$ and 1.0 . The samples were prepared by the solid-state reaction method in air at ambient pressure and heat in the $700^\circ\text{C} - 800^\circ\text{C}$ range for 48 h. By X-ray powder diffraction (XRD), we determine a solid solution until $x = 0.15$. Scanning electron microscopy (SEM) indicates that the particle size is 77 - 266 nm. The resistance measurements, as a function of temperature measurements from 7 to 300 K the $(\text{Ca}_{1-x}\text{Sr}_x)\text{RuO}_3$ system for $x = 0.0, 0.07, 0.10, 0.15$ and 1.0 show a metallic behaviour. We can even observe that the resistance of the samples is due to the partial substitution of Sr^{2+} ions and Ru ion valence. Finally, the sample $x = 0.07$ has a magnetization applied high field to 10 K, whereas that to 300 K does not have a magnetization.

Keywords

Solid-State Reaction, XRD, SEM, Electric Resistivity, Magnetic Properties

*Corresponding author.

1. Introduction

The coexistence of superconductivity and magnetic order in the rutheno-cuprates compounds like $\text{RuSr}_2\text{GdCu}_2\text{O}_8$ (Ru-1212) and their properties has been extensively studied [1]-[4]. Motivated by the discovery of high- T_c superconductivity in cuprates and the colossal magneto resistance effects in manganites, the research was initially focused on $3d$ transition-metal compounds [5]. However, as it has become increasingly clear that interesting physical phenomena of similar origin also happen in $4d$ and $5d$ electron systems, they have been getting a fair amount of attention recently. Among the $4d$ or $5d$ transition-metal compounds, ruthenium oxides probably have attracted most attention because of the discovery of superconductivity in Sr_2RuO_4 compound [6] and the potential of unique perovskite ferromagnetic metal SrRuO_3 compound [7] for thin-film applications such as tunneling magneto-resistance or ferroelectric random access memory. These ruthenites also show diverse physical properties depending on the composition or crystal structures. For example, when Sr ion is replaced by Ca ion in the above-mentioned ruthenates, the metallic and magnetic properties are significantly suppressed [8] [9]. From all these studies, it becomes evident that the preparation method plays a very important role, particularly for obtaining the different physical properties [10]. The research into electrical properties of these compounds requires very pure materials in order to optimize the particular properties of the prepared materials. In this paper, we provide information about the structural, electrical and magnetic properties of the prepared samples using the stoichiometric composition of $(\text{Ca}_{1-x}\text{Sr}_x)\text{RuO}_3$ system (CSRO) for $x = 0.0, 0.07, 0.10, 0.15$ and 1.0 .

2. Experimental Process

2.1. Synthesis

The nano-crystalline samples of the CSRO system were synthesized by solid-state reaction technique at ambient pressure. The starting materials were: RuO_2 anhydrous (99.9% STREM), SrCO_3 (99.5% CERAC) and CaCO_3 (99.99% BAKER). The structure of each reagent was corroborated by XRD. Prior to weighing, SrCO_3 and CaCO_3 were pre-heated during 10 - 20 min at 120°C , in order to be dehydrated. The stoichiometric mixture of these compounds was done in an agate mortar in air, during 15 min, resulting inhomogenous slurry. The milled polycrystals were annealed between 700°C and 800°C in a thermolyne 46,100 furnace ($\pm 4^\circ\text{C}$) during two days in air, to decompose the carbonates. The resultant nano-crystals of the samples with $0 \leq x \leq 1.0$ were compressed into pellets (diameter 13 mm thickness $1.0 - 1.5 \pm 0.05$ mm), by the application of a pressure of $1/4$ ton/cm² for 15 min in vacuum. Specimens compacted were sintered at 800°C during four days in air.

2.2. Characterization

All reagents and samples were characterized by (XRD), using a Bruker-AXS D8-Advance diffractometer with λ (CuK_α) = 1.54 \AA radiation and graphite monocromator. Diffraction patterns were collected at room temperature on the $5^\circ - 70^\circ$ in a 2θ -range with a step size of 0.017 and time per step of 397 s. The change in morphology grain size in CSRO system obtained by different heat treatments, was observed by scanning electron microscopy (SEM) on a JOEL JSM-6610LV. The micrographs 50.00 KX, were taken with a voltage of 20 KV, current intensity of 1000 pA and WD = 10 mm. The Energy Dispersive X-Ray (EDX) was performed on the same equipment equipped with an Oxford/Link System electron probe microanalyser (EPMA). The standard four-probe method with DC resistance measurement was used as a function of temperature. The system is made up in a close-cycle refrigerator tool with conventional equipment for low-level electrical measurements. Continuous monitoring of all electrical parameters during a measurements cycle allows systematic errors in the resistance values to be detected in real-time, permitting clean R vs. T profiles to be obtained with no need of additional mathematical treatment to the experimental data [11]. The magnetization was obtained on a VSM-P525 vibrating sample magnetometer. To measure the zero field-cooled (ZFC) and the field-cooled (FC) magnetization, the samples were cooled down to 2 K at zero field and 100 Oe, respectively [12]. Then the samples were measured upon heating at 100 Oe.

3. Results and Discussion

The XRD patterns of $(\text{Ca}_{1-x}\text{Sr}_x)\text{RuO}_3$ system are shown in the **Figure 1**. From those spectra, samples with $x = 0.07, 0.10$ and 0.15 show a solubility up to $x = 0.15$. Meanwhile, for $x = 0.0$ and $x = 1.0$, we observed a single

orthorhombic phase identified as CaRuO_3 PDF (70-2790) when $x = 0$, and SrRuO_3 PDF (70-2791), when $x = 1.0$ [13] [14]. The samples with $x = 0.07 - 0.15$ (that have not been reported before in the literature) show very weak reflections of a tetragonal secondary phase (identified as RuO_2 PDF (43-1027)) [15]. In the same referred samples, the Ca ion content variation shows shifts in the peaks. Then, with the calculated lattice parameters a , b , c , and the unit cell volume (V) of each of the compounds considering the following Miller index ($h k l$): (4 0 0), (0 4 0) and (0 0 4), which are shown in the following **Table 1**, can be observed that little peaks shift.

Finally, the net lattice parameters of $(\text{Ca}_{1-x}\text{Sr}_x)\text{RuO}_3$, $x = 0.0, 0.07, 0.10, 0.15$ and 1.0 system vary with the inclusion of the Sr-ion content and Ru ion coordination. Since the ionic radius of Ca^{2+} ion ($\text{Ca}^{2+} = 1.34 \text{ \AA}$) is lower than the ionic radius of Sr^{2+} ion ($\text{Sr}^{2+} = 1.44 \text{ \AA}$) [16], we conclude that the Ca ions are substituted by Sr ions with the observed unit cell variation in the volume (V) of each of the compounds, see **Table 1**. For the behavior of the lattice parameters, the solid solution has a substitution mechanism, where the Sr^{2+} ions substitute Ca^{2+} ions till $x = 0.15$. With respect to the examined diffractograms, it is worth to mention that the samples with $x = 0.0$ and $x = 1.0$ present a single orthorhombic phase identified as CaRuO_3 and SrRuO_3 , respectively. In other synthesis way to obtained this compounds reported in the literature, PDF (70-2790) and PDF (70-2791), with low temperature reaction. In contrast, the samples in the $x = 0.07 - 0.15$ range present reflections of a secondary phase identified as RuO_3 [16]. That's way the idea that the anions contributed to the formation of the mechanism of the solid solution.

The next step was the characterization of the samples achieved by SEM. The observed morphology is presented in **Figure 2**, shows considerable variations in sizes, very few secondary phases and shapes of particles. The grain size varies between 77 to 266 nm. The presented micrographs in the mentioned **Figure 2** were taken on the surface of the representative pellets of the CSRO samples with a magnification of 50 KX. Also, in some regions we observe semi-fusion that can be attributed to the ruthenium content. We can observe the secondary phase in the other gray color.

Figure 3 shows the observed resistance of the sintered materials in relation to the temperature. All the samples of $\text{Ca}_{1-x}\text{Sr}_x\text{RuO}_3$, $x = 0.0, 0.07, 0.10, 0.15$ and 1.0 system show a metallic behavior. The observed resistance in CaRuO_3 compound ($2.009 \times 10^{-2} \Omega$) is much higher than that of SrRuO_3 compound ($9.367 \times 10^{-3} \Omega$). The

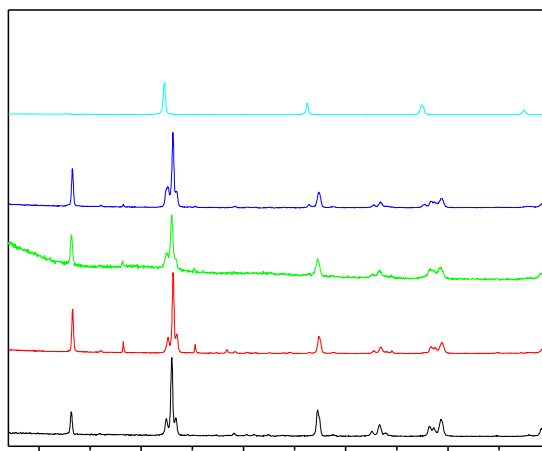


Figure 1. XRD Patterns evolution of CSRO system.

Table 1. Lattice parameters of CSRO system.

X	a (Å)	b (Å)	c (Å)	V (Å ³)
0.0	5.519(0)	7.664(9)	5.364(0)	226.9(1)
0.07	5.556(6)	7.839(8)	5.530(5)	240.9(3)
0.10	5.524(4)	7.843(8)	5.432(8)	235.4(2)
0.15	5.556(7)	7.835(1)	5.530(6)	241.0(2)
1.0	5.574(0)	7.859(4)	5.541(0)	242.7(4)

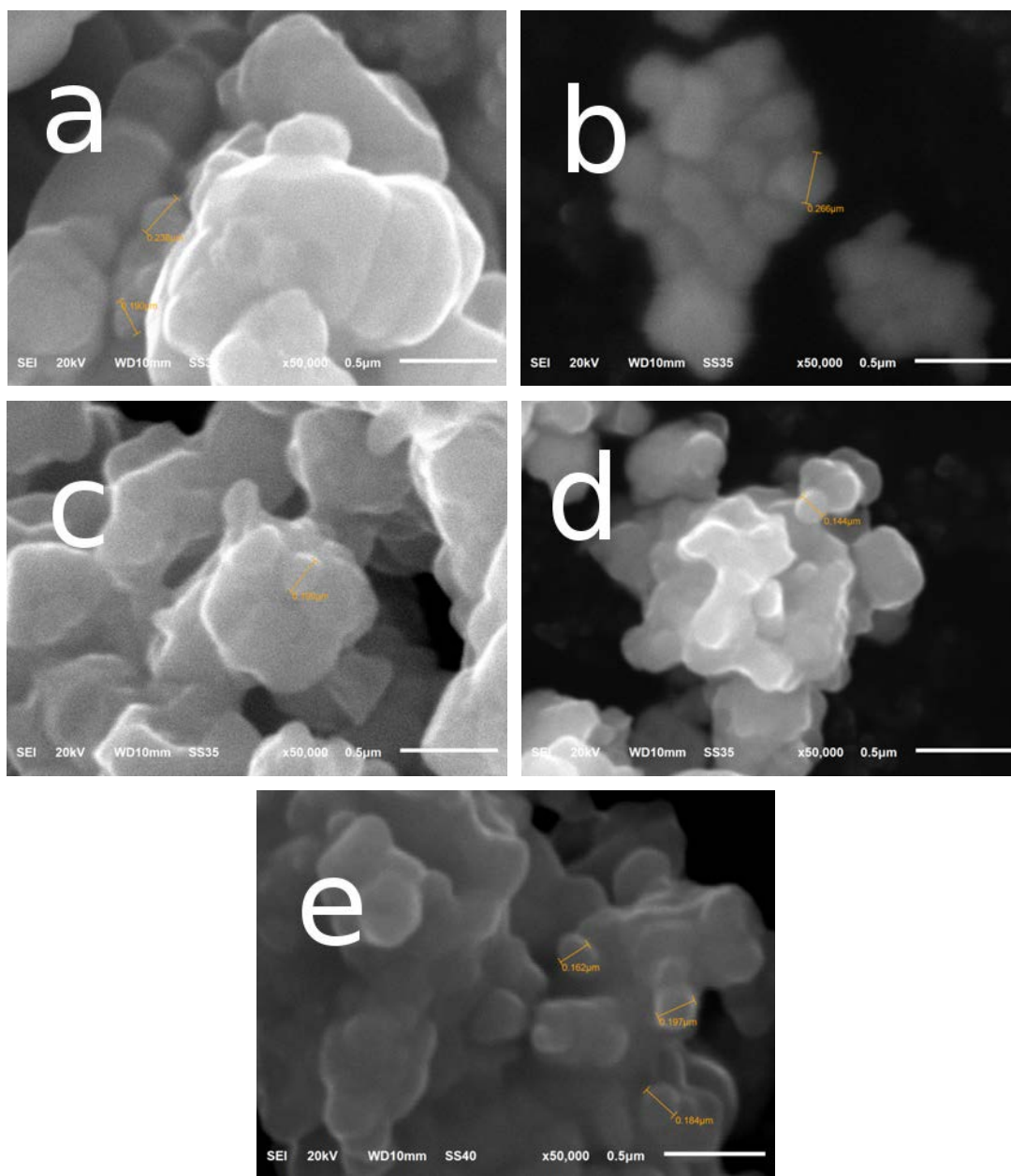


Figure 2. SEM of the CSRO system. (a) Pellet surface morphology of the CaRuO_3 sample with particle size of 190 - 238 nm; (b) Surface morphology of the $\text{Ca}_{0.93}\text{Sr}_{0.07}\text{RuO}_3$ sample with particle size of 77 - 266 nm; (c) Surface morphology of the $\text{Ca}_{0.90}\text{Sr}_{0.10}\text{RuO}_3$ sample with particle size of 199 nm; (d) Surface morphology of the $\text{Ca}_{0.85}\text{Sr}_{0.15}\text{RuO}_3$ sample with particle size of 144 nm; (e) Surface morphology of the SrRuO_3 sample with particle size of 162 - 197 nm.

CaRuO_3 compound does not exhibit ferromagnetism and its magnetic properties are still under discussion [17] together with long-range magnetic order. Moreover, as seen with the resistance curve, it does not present any anomaly in the measured range of temperature. The SrRuO_3 compound shows long-range magnetic ordering. The slope changes of 7 to 155 K, which is called Kondo effect. The temperature at which the pronounced break occurs agrees with the reported one, where T_{curie} (150 K) is related to spin scattering [18].

In the $\text{Ca}_{1-x}\text{Sr}_x\text{RuO}_3$ samples within the range of $0.07 \leq x \leq 0.15$, the short-range ferromagnetic interactions appear. This indicates that the ferromagnetism has been suppressed through the process of substitution of Sr^{2+} ions by Ca^{2+} ions. For the compounds with large Ca^{2+} ions doping ($x \geq 0.7$), no clear phase transition is discerned, and

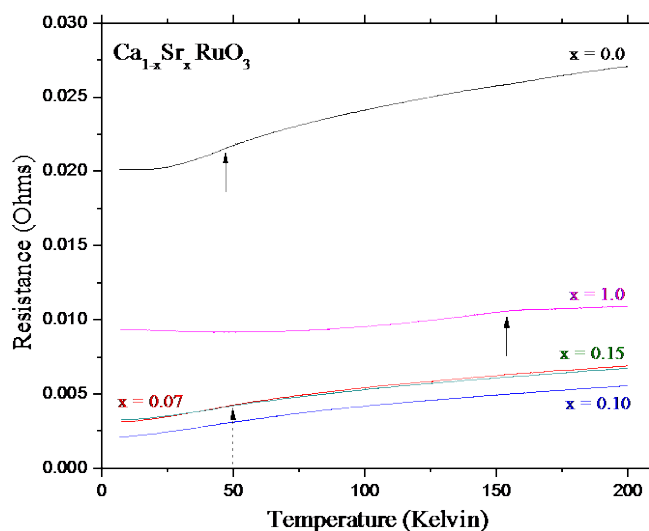


Figure 3. Temperature dependence of resistance of $\text{Ca}_{1-x}\text{Sr}_x\text{RuO}_3$. The arrows indicate the inflexions.

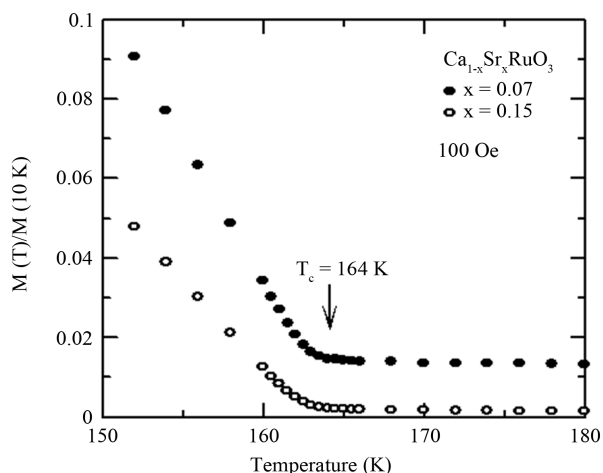


Figure 4. Magnetization measurements to 10 K ($M(T)/M(10\text{ K})$) vs curves temperature. $\text{Ca}_{1-x}\text{Sr}_x\text{RuO}_3$ samples with $x = 0.07$ and 0.15 .

only some irreversibility is observed in the magnetization curves of these materials. The disappearance of the long-range magnetic order is commonly related to the distortion of the RuO_6 octahedra associated with the partial or total replacement of Sr^{2+} ions by Ca^{2+} ions, and the corresponding narrowing of the $4d$ bandwidth [19]. The samples mentioned before show variations in each one of the profiles. This is because each one has a different chemical composition. Therefore, we can even observe that the resistance of the samples is due to the partial or total composition of Ca^{2+} ions. Since the substitution of Ca^{2+} ions for Sr^{2+} ions introduces and induces the local distortion in the vicinity of calcium ions [20] changing the Ru-O-Ru bond angle and the bandwidth, which weakens the ferromagnetism.

However, for $\text{Ca}_{1-x}\text{Sr}_x\text{RuO}_3$ ($0.07 \leq x \leq 0.15$) samples, the electrical resistance decreases with the incorporation of Sr^{2+} ions ($2.1 \times 10^{-3} \Omega$), giving less resistance than that of SrRuO_3 ($9.3 \times 10^{-3} \Omega$). With the sample preparation described above, we did not find any superconducting phase. We observe the same behaviors that were reported for other similar compounds [7] [13] [20]-[22].

The magnetization at 10 K for $x = 0.07$ and 0.15 samples are based on the application of a magnetic field of 100 Oe, as shown in Figure 4. The values T_c obtained for different samples are at a temperature of ~ 164 K, which is very close to those reported in the literature [6]. These samples exhibit such behavior because they have two

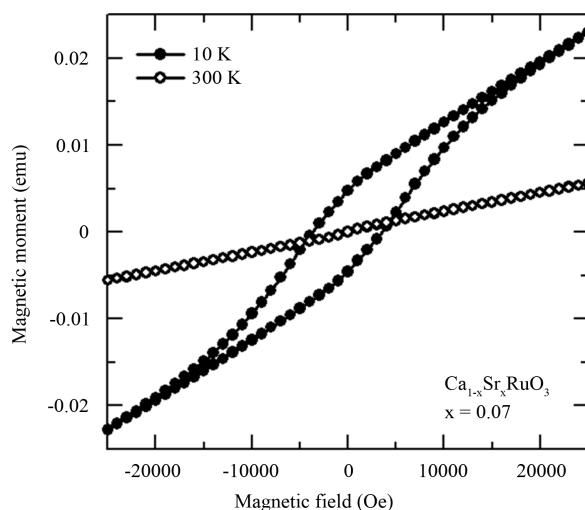


Figure 5. The curves of magnetic moment (emu) vs magnetic field (Oe) of sample $\text{Ca}_{0.93}\text{Sr}_{0.07}\text{RuO}_3$.

phases $\text{CaRuO}_3(1-x) + (\text{SrRuO}_3)(x)$, not one, which explains why both samples have the same transition FM to temperature at T_c —164 K.

Finally, as shown in **Figure 5**, we measured the magnetic moment (emu) vs. the magnetic field (Oe) for the $x = 0.07$ sample. This sample has a magnetization applied by a high field at 10 K, whereas at 300 K, it does not present magnetization. A narrow hysteresis involves a small amount of energy dissipated repeatedly, reversing the magnetization. This material could be useful in transformers and other devices for alternating current, where a zero hysteresis would be optimal.

4. Conclusion

In this work, we obtained nano-crystalline samples of CSRO system by solid-state reaction in air at room temperature, in which a solubility up to $x = 0.15$ was observed. The *SEM* micrographs exhibit an almost-spherical grain size distribution from 77 to 266 nm. We also observed that the compounds of the CSRO system exhibit metallic behavior. However, for $x = 0.07$ and 0.15, the samples exhibit a FM transition to temperature T_c at ~164 K, indicating that the transition temperature decreases with increasing Sr ions concentration. Finally, we found that the $x = 0.07$ sample has a magnetization at temperature of 10 K, whereas at 300 K the sample does not present a hysteresis behavior.

Acknowledgements

This work was partially supported by CONACYT-80380, UNAM-IN109308.

References

- [1] Bauernfeind, L., Widder, W. and Braun, H.F. (1995) Ruthenium-Based Layered Cuprates $\text{RuSr}_2\text{LnCu}_2\text{O}_8$ and $\text{RuSr}_2(\text{Ln}_{1-x}\text{Ce}_{1-x})\text{Cu}_2\text{O}_{10}$ (LnSm, Eu and Gd). *Physica C: Superconductivity*, **254**, 151-158. [http://dx.doi.org/10.1016/0921-4534\(95\)00574-9](http://dx.doi.org/10.1016/0921-4534(95)00574-9)
- [2] Bauernfeind, L., Widder, W. and Braun, H.F. (1996) Superconductors Consisting of CuO_2 and RuO_2 Layers. *Journal of Low Temperature Physics*, **105**, 1605-1610. <http://dx.doi.org/10.1007/BF00753929>
- [3] Bernard, C., Tallon, J.L., Brucher, E. and Kremer, R.K. (2000) Evidence for a Bulk Meissner State in the Ferromagnetic Superconductor $\text{RuSr}_2\text{GdCu}_2\text{O}_8$ from dc Magnetization. *Physical Review B*, **61**, Article ID: R14960.
- [4] Tallon, J.L., Bernhard, C., Bowden, M., Gilbert, P., Stoto, T., Pringle, D., et al. (1999) Coexisting Ferromagnetism and Superconductivity in Hybrid Rutheno-Cuprate Superconductors. *IEEE Transactions on Applied Superconductivity*, **9**, 1696-1699. <http://dx.doi.org/10.1109/77.784779>
- [5] Park J., Oh, J.-S., Park, J.-H., Kim, D.M. and Eom, C.-B. (2004) Electronic Structure of Epitaxial $(\text{Sr,Ca})\text{RuO}_3$ Films Studied by Photoemission and X-Ray Absorption Spectroscopy. *Physical Review B*, **69**, Article ID: 085108.

- <http://dx.doi.org/10.1103/PhysRevB.69.085108>
- [6] Maeno, Y., Hashimoto, H., Yoshida, K., Nishizaki, S., Fujita, T., Bednorz, J.G. and Lichtenberg, F. (1994) Superconductivity in a Layered Perovskite without Copper. *Nature (London)*, **372**, 532-534. <http://dx.doi.org/10.1038/372532a0>
- [7] Eom, C.B., Cava, R.J., Fleming, R.M., Phillips, J.M., van Dover, R.B., Marshall, J.H., Hus, J.W.P., Krajewski, J.J. and Peck Jr., W.F. (1992) Single-Crystal Epitaxial Thin Films of the Isotropic Metallic Oxides $\text{Sr}_{1-x}\text{Ca}_x\text{RuO}_3$ ($0 \leq x \leq 1$). *Science*, **258**, 1766. <http://dx.doi.org/10.1126/science.258.5089.1766>
- [8] Cox, P.A., Egdell, R.G., Goodenough, J.B., Hamnett, A. and Naish, C.C. (1983) The Metal-to-Semiconductor Transition in Ternary Ruthenium (IV) Oxides: A Study by Electron Spectroscopy. *Journal of Physics C: Solid State Physics*, **16**, 6221. <http://dx.doi.org/10.1088/0022-3719/16/32/014>
- [9] Shepard, M., McCall, S., Cao, G. and Crow, J.E. (1997) Thermodynamic Properties of Perovskite ARuO_3 ($A = \text{Ca}, \text{Sr}$, and Ba) Single Crystals. *Journal of Applied Physics*, **81**, 4978. <http://dx.doi.org/10.1063/1.365018>
- [10] Felner, I., Asaf, U., Reich, S. and Tsabba, Y. (1999) Magnetic Properties of $\text{RSr}_2\text{RuCu}_2\text{O}_{8+\delta}$ ($R = \text{Eu}$ and Gd). *Physica C: Superconductivity*, **311**, 163-171. [http://dx.doi.org/10.1016/S0921-4534\(98\)00642-X](http://dx.doi.org/10.1016/S0921-4534(98)00642-X)
- [11] García-Vázquez, V., Pérez-Amaro, N., Canizo-Cabrera, A., Cumplido-Espíndola, B., Martínez-Hernández, R. and Abarca-Ramírez, M.A. (2001) Selected Error Sources in Resistance Measurements on Superconductors. *Review of Scientific Instruments*, **72**, 3332. <http://dx.doi.org/10.1063/1.1386899>
- [12] <http://www.qdusa.com>
- [13] Fumihiko, F. and Tsuda, N. (1994) On the Magnetism and Electronic Conduction of Itinerant Magnetic System $\text{Ca}_{1-x}\text{Sr}_x\text{RuO}_3$. *Journal of the Physical Society of Japan*, **63**, 3798-3807. <http://dx.doi.org/10.1143/JPSJ.63.3798>
- [14] Rama Rao, M.V., Sathe, V.G., Sornadurai, D., Panigrahi, B. and Shripathi, T. (2001) Electronic Structure of ARuO_3 ($A = \text{Ca}, \text{Sr}$ and Ba) Compounds. *Journal of Physics and Chemistry of Solids*, **62**, 797-806. [http://dx.doi.org/10.1016/S0022-3697\(00\)00262-6](http://dx.doi.org/10.1016/S0022-3697(00)00262-6)
- [15] Takeda, T., Nagata, M., Kobayashi, H., Kanno, R., Kawamoto, Y., Takano, M., Kamiyama, T., Izumi, F. and Sleight, A.W. (1998) High-Pressure Synthesis, Crystal Structure, and Metal-Semiconductor Transitions in the $\text{Tl}_2\text{Ru}_2\text{O}_{7-\delta}$ Pyrochlore. *Journal of Solid State Chemistry*, **140**, 182-193.
- [16] Shannon, R.D. (1976) Revised Effective Ionic Radii and Systematic Studies of Interatomic Distances in Halides and Chalcogenides. *Acta Crystallographica A*, **32**, 751-767.
- [17] He, T. and Cava, R.J. (2001) Disorder-Induced Ferromagnetism in CaRuO_3 . *Physical Review B*, **63**, Article ID: 172403. <http://dx.doi.org/10.1103/PhysRevB.63.172403>
- [18] Gan, Q., Rao, R.A., Eom, C.B., Garrett, J.L. and Lee, M. (1998) Direct Measurement of Strain Effects on Magnetic and Electrical Properties of Epitaxial SrRuO_3 Thin Films. *Applied Physics Letters*, **72**, 978-980. <http://dx.doi.org/10.1063/1.120603>
- [19] Cao, G., McCall, S., Shepard, M., Crow, J.E. and Guertin, R.P. (1997) Thermal, Magnetic, and Transport Properties of Single-Crystal $\text{Sr}_{1-x}\text{Ca}_x\text{RuO}_3$ ($0 \leq x \leq 1.0$). *Physical Review B*, **56**, 321-329. <http://dx.doi.org/10.1103/PhysRevB.56.321>
- [20] Shikano, M., Huang, T.K., Inaguma, Y., Itoh, M. and Nakamura, T. (1994) Pressure Dependence of the Magnetic Transition Temperature for Ferromagnetic SrRuO_3 . *Solid State Communications*, **90**, 115-119. [http://dx.doi.org/10.1016/0038-1098\(94\)90942-3](http://dx.doi.org/10.1016/0038-1098(94)90942-3)
- [21] Mathieu, R., Asamitsu, A., Yamada, H., Takahashi, K.S., Kawasaki, M., Fang, Z., Nagaosa, N. and Tokura, Y. (2004) Scaling of the Anomalous Hall Effect in $\text{Sr}_{1-x}\text{Ca}_x\text{RuO}_3$. *Physical Review Letters*, **93**, Article ID: 016602. <http://dx.doi.org/10.1103/PhysRevLett.93.016602>
- [22] Pi, L., Fan, E.-H., Xiao, Y. and Zhang, Y.-H. (2006) Magnetic and Electrical Transport Properties of $\text{Sr}_{1-x}\text{La}_x\text{RuO}_3$ ($0 \leq x \leq 0.10$). *Chinese Physics Letters*, **23**, 2225-2228. <http://dx.doi.org/10.1088/0256-307X/23/8/072>

Scientific Research Publishing (SCIRP) is one of the largest Open Access journal publishers. It is currently publishing more than 200 open access, online, peer-reviewed journals covering a wide range of academic disciplines. SCIRP serves the worldwide academic communities and contributes to the progress and application of science with its publication.

Other selected journals from SCIRP are listed as below. Submit your manuscript to us via either submit@scirp.org or [Online Submission Portal](#).

